Observation of Carbodicarbene Ligand Redox Noninnocence in Highly Oxidized Iron Complexes

Siu-Chung Chan[+], Puneet Gupta[+], Xenia Engelmann, Zhi Zhong Ang, Rakesh Ganguly, Eckhard Bill, Kallol Ray, Shengfa Ye*, and Jason England*

Abstract: To probe the possibility that carbodicarbenes (CDCs) ligands are redox active ligands, we synthesized all four members of the redox series $[Fe(\mathbf{1})_2]^{n+}$ (n = 2 – 5), where **1** is a neutral tridentate CDC. Through a combination of spectroscopy and DFT calculations, we show that the electronic structure of the pentacation is $[Fe^{III}(\mathbf{1}^{\bullet+})_2]^{5+}$ (S = ½). That of $[Fe(\mathbf{1})_2]^{4+}$ is more ambiguous, but it has significant contributions from the open-shell singlet $[Fe^{III}(\mathbf{1})(\mathbf{1}^{\bullet+})]^{4+}$ (S = 0). The observed spin states derive from antiferromagnetic coupling of their constituent low-spin iron(III) centres and cation radical ligands. This marks the first time redox activity has been observed for carbones and expands the diverse chemical behaviour known for these ligands.

N-heterocyclic carbenes (NHCs) are a phenomenally successful family of ligands, in large part due to their strong σ-donor properties and chemical inertness.[1] Their utility has spurred intense efforts to explore the chemistry of carbon compounds possessing unusual valency. One of the more recent additions to this class of compounds are carbodicarbenes (CDCs), also referred to as bent allenes, which were first synthesized by the groups of Bertrand[2] and Fürstner[3] in 2008. CDCs are a subclass of carbones, the most longstanding example of which is hexaphenylcarbodiphos-phorane ($C(PPh_3)_2$).[4]

Theoretical studies have concluded that CDCs, and carbones more generally, are best regarded as coordination compounds of carbon, in which a central carbon(0) atom is coordinated by two neutral donors (**B** and **C**, Chart 1a), rather than as allenes.[5] As such, the carbone C atom possesses two essentially non-bonding pairs of electrons. This is in stark contrast to carbenes, which have a vacant p-orbital and are best regarded as carbon(II) compounds. The presence of the two non-bonding pairs of electrons in carbones has been experimentally verified by observation of germinal coordination to two distinct Lewis acids.[6]

[a] Asst. Prof. J. England, Dr. S.-C. Chan, Z. Z. Ang, Dr. R. Ganguly
Division of Chemistry and Biological Chemistry
School of Physical & Mathematical Sciences
Nanyang Technological University
21 Nanyang Link, Singapore 637371
E-mail: jengland@ntu.edu.sg
[b] Dr. S. Ye, Dr. P. Gupta
Max-Plank-Institut für Kohlenforschung
Kaiser-Wilhelm-Platz 1
D - 45470 Mülheim an der Ruhr (Germany)
E-mail: shengfa.ye@kofo.mpg.de
[c] Prof. Dr. K. Ray, X. Engelmann
Department of Chemistry
Humboldt-Universität zu Berlin
Brook-Taylor-Straße 2, 12489 Berlin (Germany)
[d] Dr. E. Bill
Max-Plank-Institut für Chemische EnergieKonversion
Stiftstraße 34 - 36
D - 45470 Mülheim an der Ruhr (Germany)
[+] These authors made contributions of equal importance

Supporting information for this article is given via a link at the end of the document.

Since the original reports of CDCs, significant efforts have been expended to elaborate their backbones in order to modulate their steric and electronic properties,[7] expand beyond the presently predominant NHC donors,[8] and to incorporate them into multidentate ligand frameworks.[9] Thus far, CDCs have mainly been utilized in stabilization of otherwise unobtainable low-coordinate main group species[10] and as surrogates for carbene ligands in various transition metal catalysed reactions.[9a, 9c, 11, 12]

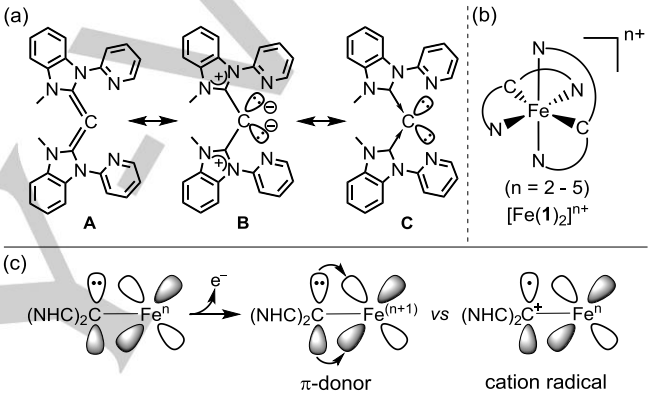

Chart 1. Resonance forms of a representative CDC, ligand **1;** b) homoleptic Fe-CDC complexes, $[Fe(\mathbf{2})_2]^{n+}$ (n = 2 – 5), reported in this work; and c) metal- versus ligand-centred oxidation in CDCs.

CDCs have been shown to be stronger σ-donor ligands than NHCs,[2] but beyond that their fundamental coordination chemistry is poorly developed. For instance, to date, there has only been one report of a first-row transition metal complex coordinated by these ligands.[13] Furthermore, carbones have primarily been used as σ-donor ligands and there has been little exploitation of the remaining "second" lone pair of electrons.[11b, 14] This includes the possibility of stabilization of high oxidation states via π-donation (i.e., M=C double bond formation), which has been invoked in only a handful of reports.[15] What has, seemingly, yet to be recognized is that the high energy of carbone lone pairs renders them potentially redox active via oxidation to radical cations.

In contrast, Fischer carbenes have long been known to be redox active. They can be reduced by 1 or 2 e^- to form the corresponding carbon-centred anion radicals and dianions.[16] These species tend to be highly reactive,[17] but have been spectroscopically characterized in several instances. More recently, it was demonstrated that cyclic (alkyl)(amino)carbenes (CAACs), which are more π-accepting than NHCs, are able to stabilize main group and transition metal compounds displaying low formal oxidation states.[18] In a noteworthy proportion of these instances, it was found that the CAAC ligands had been reduced by 1 e^- to the corresponding radicals anions.[19]

In order to probe the potential of CDCs to exhibit ligand redox noninnocence versus their ability to stabilize high oxidation states, we sought to prepare homoleptic CDC complexes of a first row transition metal (Chart 1b and 1c). To this end, we combined Ong's tridentate ligand **1**[9b] with $Fe(OTf)_2(CH_3CN)_2$. This afforded the desired complex $[Fe^{II}(\mathbf{1})_2](OTf)_2$ in good yield. X-ray crystallographic data confirmed successful tridentate coordination of **1** and formation of a homoleptic bischelate 6-coordinate complex (Figure S18). Based upon the iron-ligand bond distances (Table S2), a low-spin (S = 0) configuration can be inferred. Correspondingly, the resonances in the room temperature ^{1}H NMR spectra of $[Fe^{II}(\mathbf{1})_2]^{2+}$ are confined to the chemical shift range 4.5 – 14.0 ppm (Figure S4). This is slightly larger than expected for a truly diamagnetic complex, which combined with the broadness of the peaks is suggestive of an iron(II) complex at the lower boundary of a spin-crossover domain. The variable temperature ^{1}H NMR spectral behaviour of this complex (Figure S5) reinforce this notion.

The redox properties of $[Fe^{II}(\mathbf{1})_2]^{2+}$ was probed using cyclic voltammetry (Figures 1 and S19). Gratifyingly, three chemically reversible redox couples were observed at -0.83, 0.27 and 0.96 V (*vs* Fc^+/Fc). These are assigned to the successive 1 e^- oxidations of the $[Fe(\mathbf{1})_2]^{n+}$ dication to the corresponding tri-, tetra-, and pentacationic species. All redox couples are at accessible potentials, which allowed for synthesis of the oxidized species (n = 3 – 5) either by treatment with chemical oxidants (Scheme S1) or by bulk electrolysis. With the exception of $[Fe(\mathbf{1})_2]^{5+}$, all redox states were stable in solution and at ambient temperatures. For comparison, the free ligand **1** was studied by cyclic voltammetry and found to exhibit a single chemically irreversible anodic wave at 0.16 V (Figure S20), which we assign to oxidation to the unstable radical cation $\mathbf{1}^{\bullet+}$. Intriguingly, this is quite similar to the value for the $[Fe(\mathbf{1})_2]^{4+/3+}$ redox couple.

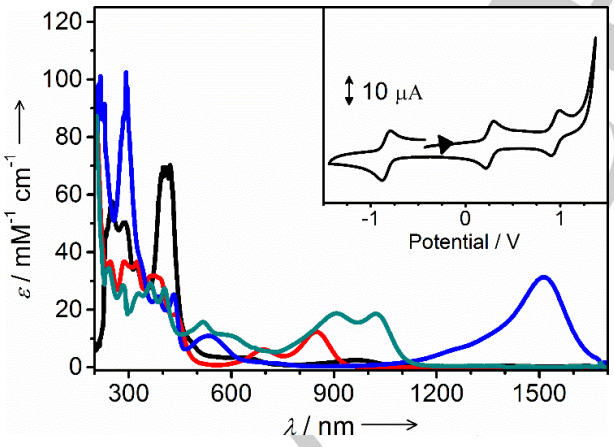

Figure 1. UV-Vis spectra of $[Fe(\mathbf{1})_2]^{n+}$ (2: black, 3: red, 4: blue, 5: green), recorded in CH_3CN solution containing 0.1 M NBu_4OTf, at 25°C. Inset: cyclic voltammogram of $[Fe^{II}(\mathbf{1})_2]^{2+}$ recorded in CH_3CN solution at 25°C, using 0.1 M NBu_4OTf as supporting electrolyte. Potentials are plotted *vs* the Fc^+/Fc redox couple. Scan rate = 100 mV s^{-1}.

All redox states of the complex show distinct UV-Vis spectral features (Figure 1, Table S3), thereby allowing straightforward monitoring of their interconversion (Figures S21 – S23). Furthermore, all of the spectra are characterized by intense charge transfer transitions, with the most unique being the near-IR feature of the tetracationic species, $[Fe(\mathbf{1})_2]^{4+}$, centred at ~1500 nm. Such a transition is typical of a ligand-to-ligand intravalence charge transfer (LLIVCT), which suggests that this complex contains a ligand cation radical ($\mathbf{1}^{\bullet+}$) and, by extension, the iron centre has a +III oxidation state.

In line with their respective stabilities, we were able to grow single crystals of $[Fe^{II}(\mathbf{1})_2](OTf)_2$, $[Fe^{III}(\mathbf{1})_2](ClO_4)_3$ and $[Fe(\mathbf{1})_2](OTf)_3(SbCl_6)$ suitable for X-ray crystallography (Table S1), but not for the pentacation $[Fe(\mathbf{1})_2]^{5+}$. These three complexes are isostructural (Figures 2 and S18); they display D_2 symmetric 6-coordinate geometries.

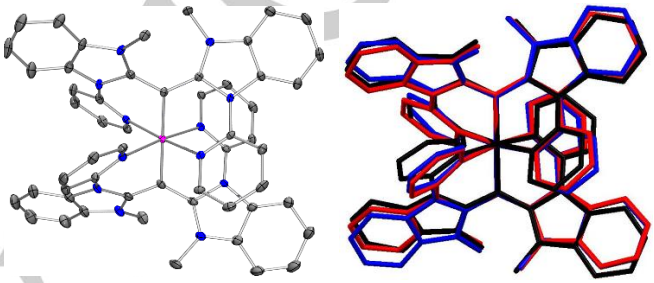

Figure 2. Left: the X-ray crystal structure of $[Fe(\mathbf{1})_2](OTf)_3(SbCl_6)$, depicted with ellipsoids at 50% probability. Atom colour scheme: carbon, grey; nitrogen, blue; iron, magenta. Right: overlay of the X-ray structures of $[Fe^{II}(\mathbf{1})_2](OTf)_2$ (red), $[Fe^{III}(\mathbf{1})_2](ClO_4)_3$ (blue), and $[Fe(\mathbf{1})_2](OTf)_3(SbCl_6)$ (black). In all cases, hydrogen atoms and counteranions have been omitted for clarity.

The Fe-ligand bond lengths seen in the dicationic and tricationic species (Table S2) are consistent with assignment as low-spin iron(II) and iron(III) complexes, respectively. Remarkably, within experimental error, the Fe-N_{py} bond distances (ranging from 1.991(4) – 2.007(2) Å) do not change upon sequential 1 electron oxidation from $[Fe^{II}(\mathbf{1})_2]^{2+}$ to $[Fe(\mathbf{1})_2]^{4+}$. This is unsurprising for the iron(II) and (III) complexes, but is not what one would expect for a "true" iron(IV) complex. In contrast, the average Fe-$C_{carbone}$ bonds decrease in length from 2.018(3) Å in $[Fe^{II}(\mathbf{1})_2]^{2+}$ to 1.968(4) Å in $[Fe^{III}(\mathbf{1})_2]^{3+}$ and 1.928(3) Å in $[Fe(\mathbf{1})_2]^{4+}$. Commensurately, the respective average $C_{carbone}$-C_{NHC} distances increased from 1.374(4) to 1.387(6) and 1.407(4) Å. These bond length changes are consistent with decreasing allenic character (Chart 1a) and the strengthening of Fe-$C_{carbone}$ bonds upon oxidation.

In all redox states, the $C_{carbone}$ atoms display sp^2 hybridization, which is ideal for π-donation of the remaining carbone lone pair to the metal centre (i.e., Fe=$C_{carbone}$ bond formation). This is evident in the C_{NHC}-$C_{carbone}$-C_{NHC} bond angles of approx. 120°, and the planarity of the Fe ion, $C_{carbone}$ donor atom, and attached C_{NHC} atoms (the deviation of these atoms from their mean plane is ≤ 0.018 Å; Table S2). Furthermore, the angles between the mean planes composed of the aforementioned atoms for the two ligands in $[Fe^{II}(\mathbf{1})_2]^{2+}$, $[Fe^{III}(\mathbf{1})_2]^{3+}$ and $[Fe(\mathbf{1})_2]^{4+}$ are 10.84°, 6.26° and 6.55°, respectively. They are not, as one might expect, orthogonal to one another. Instead, in each complex, the π-symmetry p-orbitals of both $C_{carbone}$ atoms are in the same plane and interact with a single, common d-orbital. With sufficient $C_{carbone}$-to-Fe π-donation, a d^4 electronic configuration (i.e., Fe^{IV}) would be expected to result in

an S = 0 ground state. This deviates from tetragonal oxo- and imidoiron(IV) complexes, where S = 1 spin-states dominate.

Intriguingly, the ^{1}H NMR spectrum of $[Fe(\mathbf{1})_2]^{4+}$ (Figure S6) was found to contain peaks, with well-resolved J-spin coupling, confined to the diamagnetic region. This is indicative of an S = 0 ground state. This scenario is consistent with both a complex containing iron(IV) and also iron(III) strongly antiferromagnetically coupled to a 1 e^- oxidized carbone (i.e., cation radical) ligand. It does not allow us to differentiate between these two options.

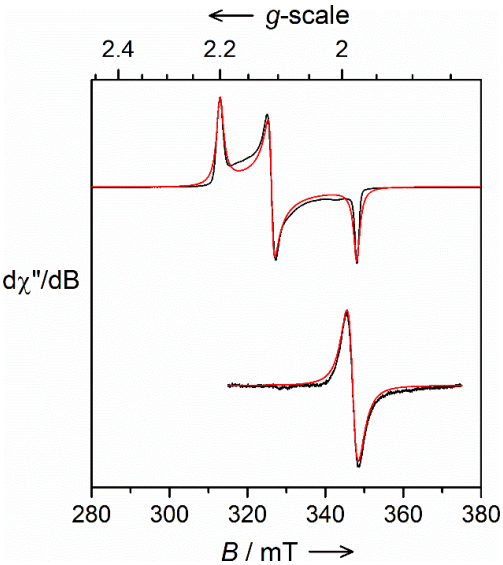

Figure 3. Perpendicular-mode X-band EPR spectra of (Top) $[Fe^{III}(\mathbf{1})_2]^{3+}$ recorded in frozen butyronitrile solution at 10 K; and (Bottom) $[Fe(\mathbf{1})_2]^{5+}$ in CH_3CN solution containing 0.1 M NBu_4PF_6, at room temperature. See Table S4 for experimental and simulation parameters.

Whereas the EPR spectra of both $[Fe^{III}(\mathbf{1})_2]^{3+}$ and $[Fe(\mathbf{1})_2]^{5+}$, recorded at 10 K, display signals characteristic of S = 1/2 ground states (Figures 3A and S25, respectively), the former is typical of low-spin iron(III) and the latter of a ligand-centred unpaired spin. More specifically, the spectrum of $[Fe^{III}(\mathbf{1})_2]^{3+}$ exhibits a signal with significant rhombicity (g_1 = 1.98, g_2 = 2.11 and g_3 = 2.20), whereas that of $[Fe(\mathbf{1})_2]^{5+}$ is only slight anisotropic (g = 1.95 – 2.05, Figure S25). Furthermore, the EPR signal of the pentacation persists in fluid solution at room temperature (Figure 3B). This is a result of slow electronic relaxation, which is incompatible with iron-centred unpaired spin. In other words, the unpaired spin must be ligand-based, which implies formation of a ligand cation radical, $\mathbf{1}^{\bullet+}$. At room temperature, it's EPR signal is isotropic and, consistent with a ligand-centred unpaired spin, its g_{iso} value of 1.98 is close to that of the free electron.

In order to elucidate the physical oxidation states of iron in $[Fe(\mathbf{1})_2]^{4+}$ and $[Fe(\mathbf{1})_2]^{5+}$, zero-field Mössbauer spectra were recorded for all members of the redox series (Figures S26 and S27, Table S5). The most reduced member $[Fe^{II}(\mathbf{1})_2]^{2+}$ exhibits a quadrupole doublet with an isomer shift (δ) of 0.42 mm s^{-1} and quadrupole splitting (ΔE_Q) of 2.20 mm s^{-1}. The moderately low δ is characteristic of low-spin iron(II), whereas the unusually large ΔE_Q is indicative of a rather anisotropic metal-ligand covalent interaction. Oxidation to $[Fe^{III}(\mathbf{1})_2]^{3+}$ resulted in a marked decrease in δ to 0.22 mm s^{-1}. This, and its ΔE_Q value of 2.24 mm s^{-1} are typical of low-spin iron(III). Crucially, further oxidation to the tetra- and pentacationic species resulted in little spectroscopic change; both have δ values of 0.16 mm s^{-1} (ΔE_Q = 2.55 and 2.37 mm s^{-1}, respectively). From this, it can be concluded that there is no increase in physical oxidation state of the metal centre, and that the +4 and +5 redox states also contain low-spin Fe^{III}.

DFT calculations were performed in order to clarify the electronic structures of $[Fe(\mathbf{1})_2]^{4+}$ and $[Fe(\mathbf{1})_2]^{5+}$. (See the supporting information for details.) Geometry optimized structures and calculated Mössbauer parameters of all members of the redox series (Tables S7 and S8, respectively) display good agreement with experiment. All redox states have frontier molecular orbitals (MOs) incorporating doubly occupied non-bonding Fe d_{x2-y2} and d_{xz} orbitals, and empty anti-bonding combinations composed primarily of Fe d_{z2} and d_{xy} orbitals (Figures S28-S31). This leaves the Fe d_{yz} orbital and the co-planar, doubly-occupied p_y orbitals of the two $C_{carbone}$ atoms, which are of appropriate symmetry for overlap with one another. Interaction of these orbitals yields π-bonding and anti-bonding (π*-orbital) combinations that have dominant ligand and metal character, respectively, plus a $C_{carbone}$-localized non-bonding molecular orbital (NBMO). The stepwise oxidation of $[Fe^{II}(\mathbf{1})_2]^{2+}$ to $[Fe(\mathbf{1})_2]^{5+}$ involves removal of electrons from these three MOs (Figure 4).

In the low-spin iron(II) complex $[Fe^{II}(\mathbf{1})_2]^{2+}$, all orbitals associated with π-bonding interactions between the $C_{carbone}$ atoms and the Fe ion are doubly occupied (Figure S28). Oxidation to $[Fe^{III}(\mathbf{1})_2]^{3+}$ proceeds via removal of an electron from the metal-centred π*-orbital, which causes slight contraction of the Fe-$C_{carbone}$ bond. Consistent with EPR measurements, this manifests in the spin-density plot as dominant localization of the unpaired spin on the Fe ion (0.91 spins, Figure S29).

Oxidation of $[Fe^{III}(\mathbf{1})_2]^{3+}$ to $[Fe(\mathbf{1})_2]^{4+}$ proceeds via removal of an second electron from the metal-centred π*-orbital. Interestingly, geometry optimization for $[Fe(\mathbf{1})_2]^{4+}$ yielded not only the expected closed-shell (RKS) solution, but also a BS(1,1) open-shell singlet that is ~3.5 kcal mol^{-1} lower in energy. The former contains a doubly occupied π-bonding orbital that has 62% Fe and 38% ligand character (Figure S30). This high level of covalency makes it difficult to assign oxidation state, but it's electronic structure can be considered a resonance hybrid of the two limiting structures $[Fe^{II}\{(\mathbf{1})_2^{2+}\}]^{4+}$ and $[Fe^{IV}(\mathbf{1})_2]^{4+}$. Thus, it approximates to Fe^{III}.

The S = 0 ground state of the open-shell solution is obtained by strong antiferromagnetic coupling (J = -630 cm^{-1}) of two electrons residing in singly-occupied molecular orbitals (SOMOs) that respectively possess 88% Fe character and 80% ligand character (Figure S30). Therefore, its electronic structure is best described as $[Fe^{III}(\mathbf{1})(\mathbf{1}^{\bullet+})]^{4+}$. Although it is tempting to conclude this is the ground state electronic structure of the complex, the close energetic proximity of the closed-shell solution prevents this. However, it is clear that the physical oxidation state of Fe in $[Fe(\mathbf{1})_2]^{4+}$ is best described as +3 and, by extension, the ligands are in a more oxidized state than in $[Fe^{III}(\mathbf{1})_2]^{3+}$.

It should be pointed out that the SOMOs in the aforementioned BS(1,1) solution derive from homolysis of the Fe-$C_{carbone}$ π-bond. Thus, although oxidation of $[Fe^{III}(\mathbf{1})_2]^{3+}$ to the tetracation is metal-centred, it does not result in a change in physical oxidation state of Fe. This can be attributed to the geometric constraints imposed

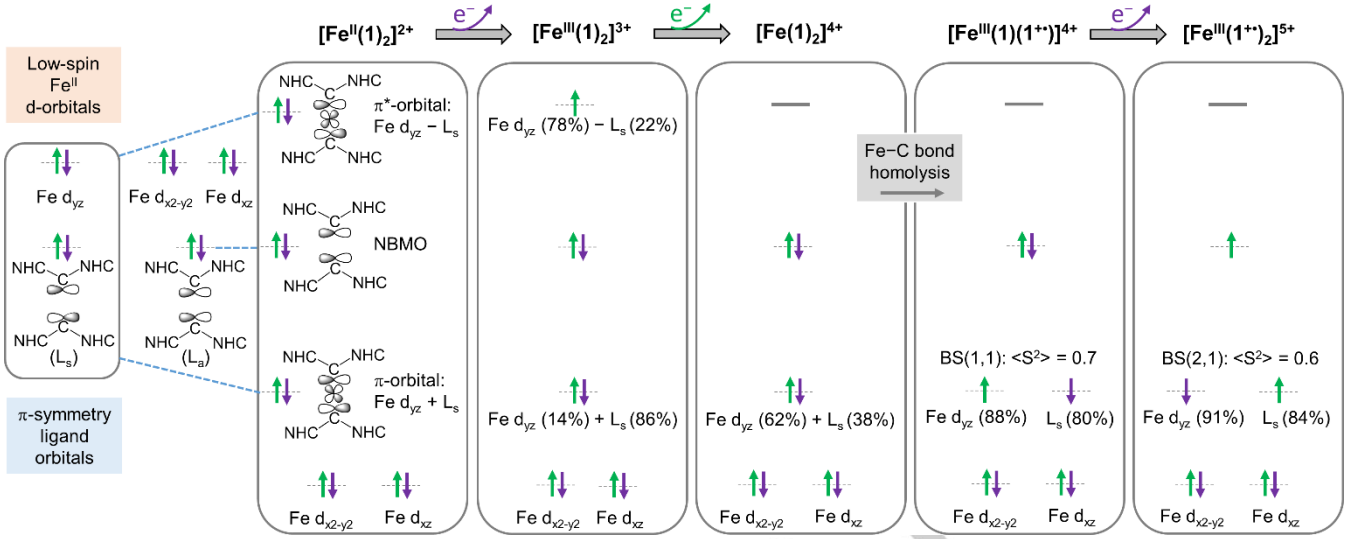

Figure 4. Schematic frontier orbital diagram depicting the electronic structures of $[Fe(\mathbf{1})_2]^{n+}$ (n = 2 – 5). L_s and L_a correspond, respectively, to the symmetric and antisymmetric combinations of the π-symmetry $C_{carbone}$-centred p-orbitals. NBMO = non-bonding molecular orbital; and $<S^2>$ = overlap integral.

by the ligand. More specifically, the depopulation of the Fe-$C_{carbone}$ π*-orbital and increase in effective nuclear charge associated with oxidation to the 4+ redox state is expected to cause a significant contraction in Fe-$C_{carbone}$ bond length. However, coordination of the flanking pyridine donors in **1** inhibits close approach of $C_{carbone}$ to the metal centre, thereby limiting Fe=C π-orbital overlap. As a consequence, homolysis of the Fe-$C_{carbone}$ π-bond is favored and only small changes in structural parameters are observed.

UKS geometry optimizations for the *S* = ½ ground state of $[Fe(\mathbf{1})_2]^{5+}$ converged to a BS(2,1) solution (Figure S31), which derives directly from the open-shell structure of the tetraction. Therein, the Fe d_{yz}-based SOMO (91% Fe character) continues to strongly antiferromagnetically couple (J = -1509 cm^{-1}) with the SOMO composed, primarily, of the symmetric linear combination of the $C_{carbone}$ p-orbitals (84% ligand character). The remaining unpaired spin is localized in the carbone-derived NBMO (100% ligand character). According to the corresponding spin density plot (Figure S31), approximately half of this NBMO is localized on the $C_{carbone}$ atom (48%, with the rest delocalized over the NHC moieties). In other words, oxidation of the tetracation involves removal of an electron from the carbone ligands and the electronic structure of the pentacation is $[Fe^{III}(\mathbf{1}^{\bullet+})_2]^{5+}$.

In conclusion, we have synthesized a homoleptic iron(II) complex of a tridentate CDC ligand, $[Fe^{II}(\mathbf{1})_2]^{2+}$ (*S* = 0), and shown that it can be oxidized stepwise by three electrons to the corresponding pentacation $[Fe(\mathbf{1})_2]^{5+}$. Based upon spectroscopic measurements and DFT calculations, it can be concluded that the first oxidation is metal-based and yields the low-spin (*S* = ½) iron(III) complex $[Fe^{III}(\mathbf{1})_2]^{3+}$, and that subsequent oxidations do not cause a further change in the physical oxidation state of the Fe. Whereas oxidation of the tetracation to the pentacation is ligand (largely, $C_{carbone}$ atom)-centred and, clearly, yields the electronic structure $[Fe^{III}(\mathbf{1}^{\bullet+})_2]^{5+}$ (*S* = ½), the situation is more ambiguous for $[Fe(\mathbf{1})_2]^{4+}$ (*S* = 0). The open-shell electronic configuration $[Fe^{III}(\mathbf{1})(\mathbf{1}^{\bullet+})]^{4+}$ is favoured, but the possibility of strong π-donation by the ligand (rather than its ionization) cannot be ruled out. Regardless, this is the first demonstration of redox noninnocence in carbone ligands and $\mathbf{1}^{\bullet+}$, thereby formed, represents a rare example of a cation radical ligand in which the unpaired spin is localized on a donor atom.[20]

Although they differ in charge, carbone cation radical ligands are isolobal with carbene radical anions. The fact that the former is accessed by oxidation and the latter by reduction, provides them with complimentary behavior. More specifically, whereas CAACs have been shown to be capable of stabilizing low oxidation states, often by reduction to radical anions, we have demonstrated that the redox activity of CDC ligands can facilitate access to high formal oxidation states. We believe the latter will be of use in facilitating multi-electron redox reactions, and that carbone cation radicals could, potentially, act as radical (e.g., H-atom) abstracting agents, which would be useful in metal-ligand cooperative reactions. Clearly, the redox noninnocence of CDCs affords a broad range of possibilities, which enhances the significant appeal of this emerging class of ligands.

Acknowledgements

JE is grateful to NTU for funding (M4081442). PG, EB and SY gratefully acknowledge the financial support of the Max-Planck Society.

Keywords: carbodicarbene • cationic ligand • iron • radical ions • redox noninnocent

[1] a) F. E. Hahn, M. C. Jahnke, *Angew. Chem. Int. Ed.* **2008**, *47*, 3122; b) M. Melaimi, M. Soleilhavoup, G. Bertrand, *Angew. Chem. Int. Ed.* **2010,** *49*, 8810; c) M. N. Hopkinson, C. Richter, M. Schedler, F. Glorius, *Nature* **2014**, *510*, 485.

[2] C. A. Dyker, V. Lavallo, B. Donnadieu, G. Bertrand, *Angew. Chem. Int. Ed.* **2008**, *47*, 3206.

[3] a) A. Fürstner, M. Alcarazo, R. Goddard, C. W. Lehmann, *Angew. Chem. Int. Ed.* **2008**, *47*, 3210; b) M. Alcarazo, C. W. Lehmann, A. Anoop, W. Thiel, A. Fürstner, *Nat. Chem.* **2009**, *1*, 295.

[4] F. Ramirez, N. B. Desai, B. Hansen, N. McKelvie, *J. Am. Chem. Soc.* **1961**, *83*, 3539.

[5] a) R. Tonner, F. Öxler, B. Neumüller, W. Petz, G. Frenking, *Angew. Chem. Int. Ed.* **2006**, *45*, 8038; b) R. Tonner, G. Frenking, *Angew. Chem. Int. Ed.* **2007**, *46*, 8695; c) R. Tonner, G. Frenking, *Chem. Eur. J.* **2008**, *14*, 3260; d) R. Tonner, G. Frenking, *Chem. Eur. J.* **2008**, *14*, 3273; e) R. Tonner, G. Heydenrych, G. Frenking, *Chemphyschem,* **2008**, 9, 1474; f) S. Klein, R. Tonner, G. Frenking, *Chem. Eur. J.* **2010**, *16*, 10160.

[6] a) H. Schmidbaur, O. Gasser, *Angew. Chem. Int. Ed.* **1976**, *15*, 502; b) J. Vicente, A. R. Singhal, P. G. Jones, *Organometallics* **2002**, *21*, 5887; c) W. Petz, F. Öxler, B. Neumüller, R. Tonner, G. Frenking, Eur. J. Inorg. Chem. **2009**, 4507.

[7] a) O. Kaufhold, F. E. Hahn, *Angew. Chem. Int. Ed.* **2008**, *47*, 4057; b) W.-C. Chen, Y.-C. Hsu, C.-Y. Lee, G. P. A. Yap, T.-G. Ong, *Organometallics* **2013**, 32, 2435; c) W.-C. Chen, J.-S. Shen, T. Jurca, C.-J. Peng, Y.-H. Lin, Y.-P. Wang, W.-C. Shih, G. P. A. Yap, T.-G. Ong, *Angew. Chem. Int. Ed.* **2015**, *54*, 15207; d) W.-C. Shih, Y.-T. Chiang, Q. Wang, M.-C. Wu, G. P. A. Yap, L. Zhao, T.-G. Ong, *Organometallics*, **2017**, *36*, 4287; e) S.-K. Liu, W.-C. Shih, W.-C. Chen, T.-G. Ong, *ChemCatChem* **2018**, *10*, 1483.

[8] a) V. Lavallo, C. A. Dyker, B. Donnadieu, G. Bertrand, *Angew. Chem. Int. Ed.* **2008**, *47*, 5411; b) V. Lavallo, C. A. Dyker, B. Donnadieu, G. Bertrand, *Angew. Chem. Int. Ed.* **2009**, *48*, 1540; c) I. Fernández, C. A. Dyker, A. DeHope, B. Donnadieu, G. Frenking, G. Bertrand, *J. Am. Chem. Soc.* **2009**, *131*, 11875; d) D. A. Ruiz, M. Melaimi, G. Bertrand, *Chem. Asian J.* **2013**, *8*, 2940; e) C. Pranckevicius, L. Liu, G. Bertrand, D. W. Stephan, *Angew. Chem. Int. Ed.* **2016**, *55*, 5536.

[9] a) M. J. Goldfogel, C. C. Roberts, S. J. Meek, *J. Am. Chem. Soc.* **2014**, *136*, 6227; b) Y.-C. Hsu, J.-S. Shen, B.-C. Lin, W.-C. Chen, Y.-T. Chan, W.-M. Ching, G. P. A. Yap, C.-P. Hsu, T.-G. Ong, *Angew. Chem. Int. Ed.* **2015**, *54*, 2420; c) J. S. Marcum, C. C. Roberts, R. S. Manan, T. N. Cervarich, S. J. Meek, *J. Am. Chem. Soc.* **2017**, *139*, 15580.

[10] a) W.-C. Chen, C.-Y. Lee, B.-C. Lin, Y.-C. Hsu, J.-S. Shen, C.-P. Hsu, G. P. A. Yap, T.-G. Ong, *J. Am. Chem. Soc.* **2014**, *136*, 914; b) N. Đorđević, R. Ganguly, M. Petković, D. Vidović, *Chem. Commun.* **2016**, *52*, 9789; c) N. Đorđević, R. Ganguly, M. Petković, D. Vidović, *Inorg. Chem.* **2017**, *56*, 14671.

[11] a) C. Pranckevicius, L. Fan, D. W. Stephan, *J. Am. Chem. Soc.* **2015**, *137*, 5582; b) C. C. Roberts, D. M. Matías, M. J. Goldfogel, S. J. Meek, *J. Am. Chem. Soc.* **2015**, *137*, 6488; c) M. J. Goldfogel, S. J. Meek, *Chem. Sci.* **2016**, *7*, 4079; d) A. L. Liberman-Martin, R. H. Grubbs, *Organometallics* **2017**, *36*, 4091; e) M. J. Goldfogel, C. C. Roberts, R. S. Manan, S. J. Meek, *Org. Lett.* **2017**, *19*, 90.

[12] Y.-C. Hsu, V. C.-C. Wang, K.-C. Au-Yeung, C.-Y. Tsai, C.-C. Chang, B.-C. Lin, Y.-T. Chan, C.-P. Hsu, G. P. A. Yap, T. Jurca, T.-G. Ong, *Angew. Chem. Int. Ed.* **2018**, *57*, 4622.

[13] C. Pranckevicius, D. W. Stephan, *Organometallics* **2013**, *32*, 2693.

[14] W.-C. Chen, W.-C. Shih, T. Jurca, L. Zhao, D. M. Andrada, C.-J. Peng, C.-C. Chang, S.-K. Liu, Y.-P. Wang, Y.-S. Wen, G. P. A. Yap, C.-P. Hsu, G. Frenking, T.-G. Ong, *J. Am. Chem. Soc.* **2017**, *139*, 12830.

[15] a) J. Sundermeyer, K. Weber, K. Peters, H. G. von Schnering, *Organometallics* **1994**, *13*, 2560; b) A. E. Bruce, A. S. Gamble, T. L. Tonker, J. L. Templeton, *Organometallics* **1987**, *6*, 1350.

[16] a) P. J. Krusic, U. Klabunde, C. P. Casey, T. F. Block, *J. Am. Chem. Soc.*, **1976**, *98*, 2015; b) S. Lee, N. J. Cooper, *J. Am. Chem. Soc.* **1990**, *112*, 9419.

[17] a) M. A. Sierra, M. G.-Gallego, R. M.-Álvarez, *Chem. Eur. J.* **2007**, *13*, 736; b) M. P. Doyle, Angew. Chem. Int. Ed. **2009**, *48*, 850; c) W. I. Dzik, X. P. Zhang, B. de Bruin, *Inorg. Chem.* **2011**, *50*, 9896; d) V. Lyaskovskyy, B. de Bruin, *ACS catal*, **2012**, *2*, 270; e) C. te Grotenhuis, B. de Bruin, *Synlett*., **2018**, doi: 10.1055/s-0037-1610204.

[18] a) M. Soleihavoup, G. Bertrand, *Acc. Chem. Res.* **2015**, *48*, 256: b) S. Roy, K. C. Mondal, H. W. Roesky, *Acc. Chem. Res.* **2016**, *49*, 357; c) K. C. Mondal, S. Roy, H. W. Roesky, *Chem. Soc. Rev.* **2016**, *45*, 1080; d) M. M. Melaimi, R. Jazzar,M. Soleihavoup, G. Bertrand, *Angew. Chem. Int. Ed.* **2017**, *56*, 10046.

[19] a) K. C. Mondal, H. W. Roesky, M. C. Schwarzer, G. Frenking, I. Tkach, H. Wolf, D. Kratzert, R. Herbst-Irmer, B. Niepötter, D. Stalke, *Angew. Chem. Int. Ed.* **2013**, *52*, 1801; b) P. P. Samuel, K. C. Mondal, H. W. Roesky, M. Hermann, G. Frenking, S. Demeshko, F. Meyer, A. C. Stückl, J. H. Christian, N. S. Dalal, L. Ungur. L. F. Chibotaru, K. Pröpper, A. Meents, B. Dittrich, *Angew. Chem. Int. Ed.* **2013**, *52*, 11817; c) K. C. Mondal, P. P. Samuel, M. Tretiakov, A. P. Singh, H. W. Roesky, A. C. Stückl, B. Niepötter, E. Carl, H. Wolf, R. Herbst-Irmer, D. Stalke, *Inorg. Chem.* **2013**, *52*, 4736; d) D. S. Weinberger, M. Melaimi, C. E. Moore, A. L. Rheingold, G. Frenking, P. Jerabek, G. Bertrand, *Angew. Chem. Int. Ed.* **2013**, *52*, 8964; e) A. P. Singh, P. P. Samuel, H. W. Roesky, M. C. Schwarzer, G. Frenking, N. S. Sidhu, B. Dittrich, *J. Am. Chem. Soc,* **2013**, *135*, 7324; f) D. S. Weinberger, N. Amin SK, K. C. Mondal, M. Melaimi, G. Bertrand, A. C. Stückl, H. W. Roesky, B. Dittrich, S. Demeshko, B. Schwederski, W. Kaim, P. Jerabek, G. Frenking, *J. Am. Chem. Soc.* **2014**, *136*, 6235; g) M. Arrowsmith, J. Böhnke, H. Braunschweig, M. A. Celik, C. Claes, W. C. Ewing, I. Krummenacher, K. Lubitz, C. Schneider, *Angew. Chem. Int. Ed.* **2016**, *55*, 11271.

[20] a) W. Matheis, W. Kaim, *J. Chem. Soc. Faraday Trans.* **1990**, *86*, 3337; b) H. Helten, C. Neumann, A. Espinosa, P. G. Jones, M. Nieger, R. Streubel, *Eur. J. Inorg. Chem.* **2007**, 4669.

Entry for the Table of Contents

COMMUNICATION

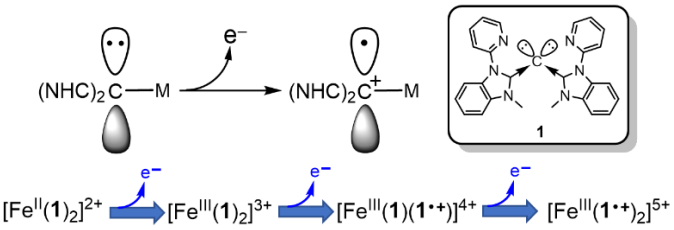

Carbones contain C atoms possessing two lone pairs of electrons. Thus, in addition to σ-coordination to a metal ion, they have a further pair of electrons rendering them capable of π-donation or germinal coordination to a second metal. We show via formation of a $[Fe(\mathbf{1})_2]^{n+}$ (n = 2-5) redox series, where **1** is a tridentate carbodicarbene ligand, that this 2nd pair of electrons allows them to be redox active.

Siu-Chung Chan, Puneet Gupta, Xenia Engelmann, Zhi Zhong Ang, Rakesh Ganguly, Eckhard Bill, Kallol Ray, Shengfa Ye, and Jason England**

Page No. – Page No.

Observation of Carbodicarbene Ligand Redox Noninnocence in Highly Oxidized Iron Complexes

[a] Asst. Prof. J. England, Dr. S.-C. Chan, R. Ganguly
Division of Chemistry and Biological Chemistry
School of Physical & Mathematical Sciences
Nanyang Technological University
21 Nanyang Link
Singapore 637371
E-mail: jengland@ntu.edu.sg
[b] Dr. S. Ye, Dr. P. Gupta